Sub-Synchronous Interaction Damping Control for DFIG Wind Turbines

Andres E. Leon, *Member, IEEE*, and Jorge A. Solsona, *Senior Member, IEEE*

***Abstract*—This paper presents a damping control to mitigate sub-synchronous interactions (SSI) in doubly-fed induction generator (DFIG) wind turbines connected to series-compensated lines. This issue has gained attention due to the recent SSI phenomena reported in DFIG wind farms located near series capacitors. Two approaches which add a supplementary damping control signal are compared: one of them, integrated to the grid-side converter, and the other one, to the rotor-side converter. The SSI damping controls are designed using a multi-input multi-output state-space methodology. This allows to easily tune a high performance controller using several measurements and control inputs. Small- and large-signal stability analyses, robustness aspects, impact of the supplementary controls on the system modes, and influence of different operating conditions on the SSI are also discussed. The obtained results show that the supplementary control is able to properly damp the sub-synchronous oscillations of DFIG wind turbines by updating the existing DFIG control systems without the inclusion of expensive additional damping devices, and reducing the risk of wind generation tripping.**

***Index Terms*—Resonance mitigation, series compensation, subsynchronous control interactions (SSCI), subsynchronous resonance (SSR), wind energy conversion systems (WECS).**

I. Introduction

WIND power plants are rapidly increasing in number and being located in areas with favorable wind conditions, usually far from load centers [1]. This additional wind power generation can be accommodated either by building new transmission lines or by enhancing the power transfer capability of the existing lines using series compensation [2]. Series capacitor compensation is being increasingly considered because it is a well-known technology and a cost-effective solution to enhance the transient stability and power transmission capacity of the required corridors [3]. Several wind farms in the United States and Canada are expected to be, or already are, connected to series-compensated lines to evacuate bulk power from wind resources [4]. However, series capacitor compensation can produce adverse effects such as sub-synchronous interactions (SSI) with other power system components [5].

Manuscript received November 09, 2013; revised February 19, 2014 and April 30, 2014; accepted May 26, 2014. Date of publication June 10, 2014; date of current version December 18, 2014. This work was supported by Consejo Nacional de Investigaciones Científicas y Técnicas (CONICET) and Universidad Nacional del Sur. Paper no. TPWRS-01443-2013.

The authors are with the Instituto de Investigaciones en Ingeniería Eléctrica (IIIE) "Alfredo Desages" (UNS-CONICET), Universidad Nacional del Sur (DIEC-UNS), Bahía Blanca, Argentina (e-mail: aleon@iiie-conicet.gob.ar).

Color versions of one or more of the figures in this paper are available online at http://ieeexplore.ieee.org.

Digital Object Identifier 10.1109/TPWRS.2014.2327197

Recently, two SSI incidents between doubly-fed induction generator (DFIG) wind farms and series-compensated lines caught the attention of system operators and the research community. In the first event, in the southern Electric Reliability Council of Texas (ERCOT) system, a 345-kV transmission line was tripped after a fault and, subsequently, the wind farm became radially connected to a 50% series-compensated line. As a result, the system experienced both over-voltages and growing sub-synchronous oscillations (SSO), causing equipment damage [6]–[9]. The second event, in southwestern Minnesota, was in a 150-MW DFIG wind farm connected to a 60% series-compensated line, also reporting growing SSO that were not detected by conventional relays [10].

Several studies on SSI considering series-compensated wind farms based on squirrel-cage induction generators [4], [11] and DFIG [2], [12]–[17] have recently been performed, but only analysis of the SSI has been accomplished. As countermeasures for these SSI, it can be mentioned: 1) detection algorithms to trip the wind generators [6], [10], 2) bypass filters across the series capacitor [5], 3) approaches using flexible ac transmission systems (FACTS) (for example, thyristor-controlled series capacitor (TCSC) [3] and static synchronous compensator (STATCOM) [18], [19]), and 4) modifications of wind turbine control systems (like power converter controls available in DFIG wind turbines). The last solution is the most suitable from an economic point of view, because it avoids the installation of expensive additional damping devices, such as FACTS or bypass filters [5], [9].

Countermeasures based on control system modifications are cheap, avoid generator tripping, and can be quickly implemented. Two approaches can be considered for DFIG wind turbines: one of them adds an SSI damping control signal in the reactive current control loop of the grid-side converter (GSC) [20]–[22] (as in a STATCOM scheme), whereas the other one adds the damping control signal in the rotor voltage through the rotor-side converter (RSC) [23]. A second distinction can also be made, depending on whether SSI damping controls use either local or remote measurements. Until the present time, only a few SSI mitigation solutions based on modifications of the DFIG wind turbine control system are found in the literature [20]–[23]. However, these proposals only consider simple proportional controls or lead-lag compensators with one measurement and one control input. These single-input single-output (SISO) control approaches do not take the performance advantages of using several measurements and multiple control inputs. Multi-input multi-output (MIMO) approaches are attractive to consider because they present more degrees

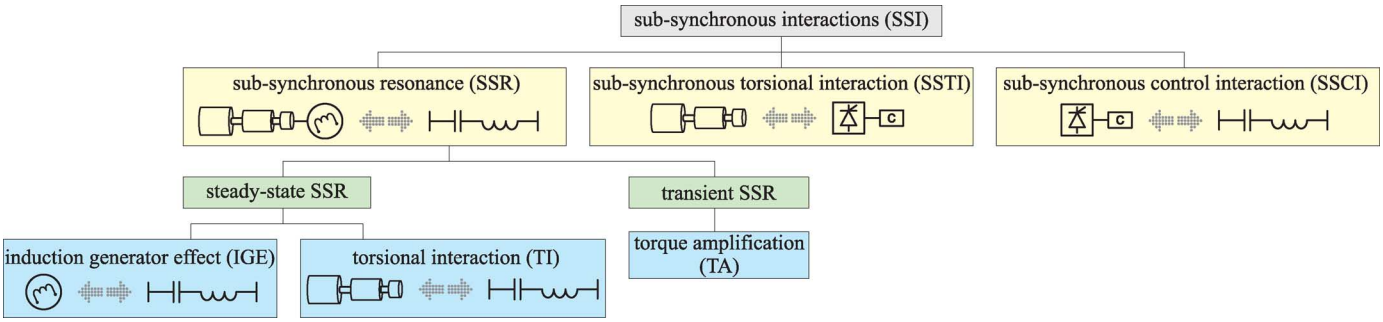

Fig. 1. Classification of the sub-synchronous interactions.

of freedom in the control design and, therefore, higher performance and robustness can be obtained.

The main contributions of this paper are: 1) SSI mitigation in DFIG wind farms by adding a supplementary damping control designed using a MIMO state-space approach, 2) comparison of the GSC and RSC control loops to perform the SSI damping action, and 3) small- and large-signal stability analysis to thoroughly describe and assess the performance and robustness of the base scenario and controlled cases over a wide range of operating conditions. Additionally, the proposed auxiliary damping control is integrated to the existing converter vector controls without removing them. In this way, it could be more acceptable for system operators and manufactures who are usually conservative to fully replace the well-known PI control structures.

II. Background

In this section, different definitions are introduced and discussed to better explain the SSI phenomena. Formally, *SSI is a general term that defines two power system elements exchanging energy with each other at one or more of the natural frequencies of the combined system below the synchronous frequency* [6]. According to the different elements involved (*e.g.,* series capacitor, generator, mechanical system, power electronic control), the SSI can be classified into [6], [23]–[25]: sub-synchronous resonance (SSR), sub-synchronous torsional interaction (SSTI) and sub-synchronous control interaction (SSCI). Fig. 1 shows the different SSI categories.

A. Sub-Synchronous Resonance

SSR is a condition where a series capacitor compensated system exchanges significant energy with a turbine-generator at a frequency below the synchronous frequency [26]. In a radial series-compensated power system, the electrical resonance frequency is given by

$$f_{er} = \pm f_s \sqrt{\frac{x_c}{x_L}} \tag{1}$$

where f_s is the synchronous frequency, x_c is the reactance of the series capacitor, and x_L is the total reactance of the transmission line, transformers, and generator. Small disturbances excite stator currents at frequencies $\pm f_{er}$, and the positive-sequence component of these currents produce a stator flux at frequency f_{er}. Consequently, currents in the rotor winding will be induced at the complementary frequency $f_r = f_o - f_{er}$, where f_o is the rotor electrical frequency. These rotor currents result in sub-synchronous stator voltage components which may enhance the stator currents to produce a self-excitation phenomenon [3]. On the other hand, the interaction of the aforementioned stator flux, rotating at sub-synchronous frequency f_{er}, with the rotor dc flux, rotating at frequency f_o, develops an electromagnetic torque at a frequency $f_r = f_o - f_{er}$[26]. If the frequency f_r of this torque component is close to a mechanical natural frequency of the drive-train system, torsional interactions can produce undamped oscillations between the drive-train and the electrical network.

The SSR is a classical problem mainly associated to conventional synchronous machines (*e.g.*, thermal power plants) closely connected to series-compensated transmission lines; however, such interaction is also possible in wind power plants, as anticipated by the pioneer work [27].

There are two types of SSR phenomena [28]: first, the self-excitation or steady-state SSR [involving both induction generator effect (IGE) and torsional interaction (TI)], and second, the transient SSR [or shaft torque amplification (TA)].

1) Induction Generator Effect: Self-excitation of a series capacitor compensated system alone, assuming constant rotor speed, is caused by induction generator effect [26]. The IGE involves only the electric machine with the network, but not the turbine mechanical system. That is, if the rotor is considered to be rigid, only the IGE phenomenon is present.

From the point of view of a sub-synchronously rotating stator flux, the synchronous generator acts as an induction machine [5]. Consequently, for both synchronous and induction machines, the slip at the sub-synchronous frequency is

$$s_{ssr} = \frac{f_{er} - f_o}{f_{er}}. \tag{2}$$

From the equivalent circuit of an induction machine, the equivalent rotor resistance at the sub-synchronous frequency is given by [13]

$$R_{eq}^{ssr} = \frac{R_r'}{s_{ssr}}. \tag{3}$$

If the rotating stator flux at frequency f_{er}, produced by the sub-synchronous stator currents, is slower than the rotor electrical frequency $f_{er} < f_o$, the rotor-side resistance R_{eq}^{ssr} will be negative (viewed from the stator terminals) [3], [13], [19]. When the magnitude of the resistance R_{eq}^{ssr} exceeds the sum

of the stator and network resistances, the system has a negative damping at the sub-synchronous frequency, and growing voltage and current oscillations will be experienced.

In a DFIG wind turbine, the electrical resonance frequency f_{er} is usually lower than the rotor frequency f_o, and the slip s_{ssr} is negative. When the wind speed increases, the corresponding optimal rotor frequency f_o also increases, and the slip is more negative and larger. Accordingly, the absolute value of the equivalent negative resistance R_{eq}^{ssr} decreases and, therefore, there is more damping for the SSO; the opposite happens when the wind speed decreases. On the other hand, when the compensation level increases, the frequency f_{er} increases as well, and the slip is less negative and smaller. As a result, the absolute value of R_{eq}^{ssr} will increase, reducing the SSO damping [22], [29].

2) Torsional Interaction: TI is the interaction between the turbine-generator mechanical system and a series-compensated electrical network [26]. The turbine-generator shaft responds to power system disturbances with oscillations at its torsional resonance (or natural) frequencies f_n. These rotor torsional oscillations rendering to the generator terminals produce stator voltage components at the frequencies $f_{en} = f_o \pm f_n$. When the sub-synchronous frequency $f_{en} = f_o - f_n$ of the voltage component is close to an electrical resonance frequency f_{er} of the network, the resulting stator current produces a flux and, consequently, a torque which reinforces (or mutually excites) the rotor torsional modes.

This can produce large magnitude torques and sustained or growing oscillations which can lead to fatigue damage, lifetime reduction, and even failures in turbine-generator shafts [26]. Finally, the TI phenomenon involves both electrical and mechanical dynamics, and may occur when the electrical resonant frequency f_{er} is near the complement of one of the torsional resonance frequencies f_n of the mechanical drive-train system [3]. The TI oscillation frequencies are fixed and determined by the known torsional modes of the turbine-generator shaft.

As wind turbines present several mechanical modes related to turbine blades, shaft, gear box, tower, etc. [3], [27], the TI phenomena may be of concern in these cases. However, lightly-damped torsional modes in wind turbines are generally at low frequencies, which should not be a problem because high series compensation levels are required to reach these mechanical resonance modes [2], [11], [13], [25].

3) Torque Amplification: Following a significant disturbance in a series capacitor compensated system, the resulting electromagnetic torque on the machine rotor oscillates at a frequency $f_r = f_o - f_{er}$. If this frequency is near a torsional resonance frequency f_n, the generated transient shaft torques could be much larger than those produced by the same disturbance in a system without series capacitors. Higher torques can also result if the fault duration time (or clearing time of fault) reinforces the initial transient response [26].

B. Sub-Synchronous Torsional Interaction

SSTI defines the problem of a turbine-generator near a power electronic controller when the mechanical system resonates with the negative damping of the controller at sub-synchronous frequencies [6], [25]. Power electronic controllers (such as those in HVDC links, FACTS, and any control device that responds rapidly to power variations in the sub-synchronous frequency range) can exhibit negative damping at sub-synchronous frequencies, which can cause undamped oscillations in the fixed mechanical torsional modes of drive-train systems [23], [30]. The SSTI is also included in the category of device-dependent sub-synchronous interactions [26].

C. Sub-Synchronous Control Interaction

SSCI is an interaction between a power electronic control system and a series-compensated electrical network [6], [25]. The SSCI is not related to the mechanical shaft system, and neither TI nor SSTI phenomena are involved, so the resonance frequency is not fixed, changing under different system conditions and converter control algorithms [9]. If protective measures are not considered, SSCI oscillations can build-up quickly, compared with mechanical interactions, because they are a purely control/electrical phenomenon [23], [25], [30].

SSI events have recently shown that control systems associated with DFIG wind turbines can present a negative resistance to the grid under sub-synchronous conditions [1], [5], [7]. This problem arises over a wide range of slip frequencies, and is primarily caused by the fast action of the rotor current control loop, which produces an effective increase in the rotor-side resistance; because of the described physics of the rotating machines, this is seen as a negative resistance from the stator perspective [1]. Therefore, it is not the traditional IGE phenomenon [6].

Full-converter wind turbines have not exhibited SSCI problems [1], [5], [25], because the GSC decouples the machine from the sub-synchronous network resonances [31].

III. DFIG Wind Farm Modeling

In our study, the wind farm was represented by an aggregated model, using the weighted average impedance method [4], [11], [32]. This approach provides a reasonable approximation, and it is common practice in this kind of studies [2], [9], [15], [24]. The DFIG model consists of the three-phase stator and rotor windings (equations taken from [33]), the back-to-back voltage-source converters [34], the power curve of the wind turbine [35], and the mechanical drive-train system represented by a six-mass model [36], [37]. To calculate the eigenvalues in the modal analysis, an average dynamic model of the voltage-source converters was considered [34]. The network transmission lines were represented with electromagnetic transient models using equivalent π circuits [38]. The parameters of the electrical network were extracted from [6]–[9], and shown in Fig. 2.

Fig. 3 shows a block diagram of the considered DFIG converter controllers, where we described both the inner current control loops and the outer control loops (*e.g.,* maximum power point tracking (MPPT) technique, ac terminal voltage control, and dc-link voltage regulation). The MPPT algorithm was implemented through the current-mode control scheme, which measures the rotor speed and uses the turbine power-speed characteristic to obtain the optimal active power reference (see further details in [39]). The terminal voltage was regulated by the DFIG reactive current loop via a control with slope (or droop control) [40], and the dc-link voltage was controlled

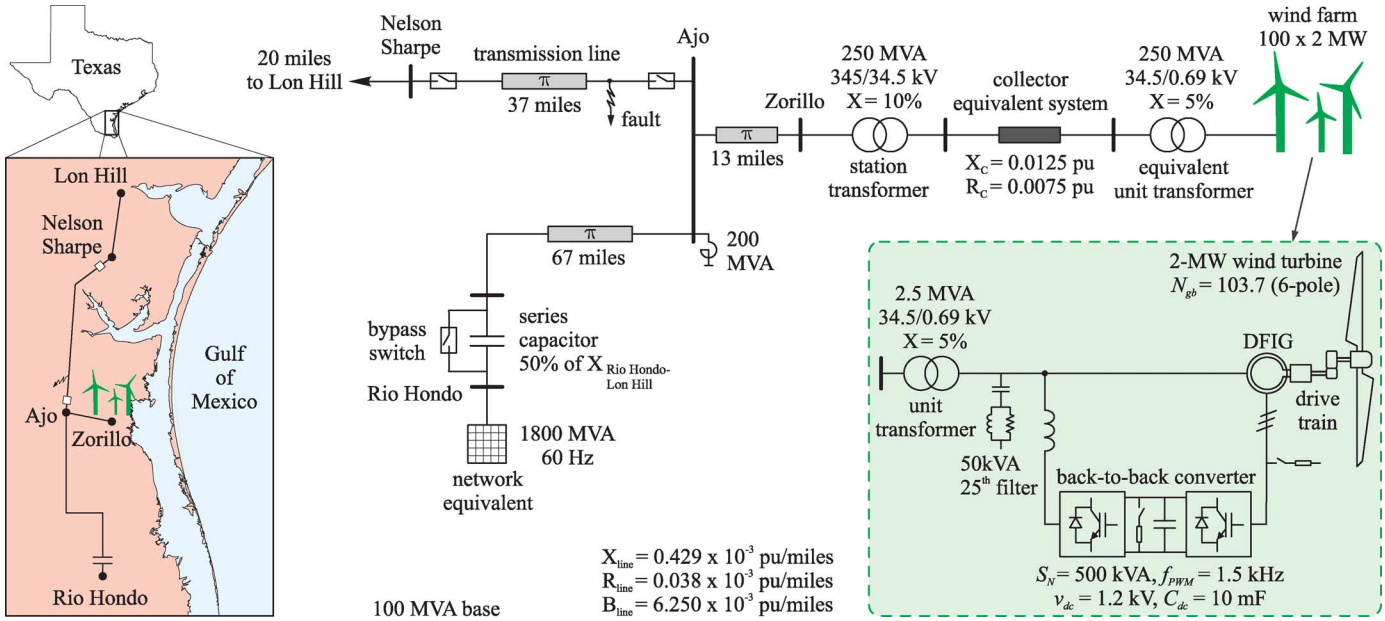

Fig. 2. Portion of the series-compensated transmission system in the south of Texas that experienced sub-synchronous oscillations in October 2009.

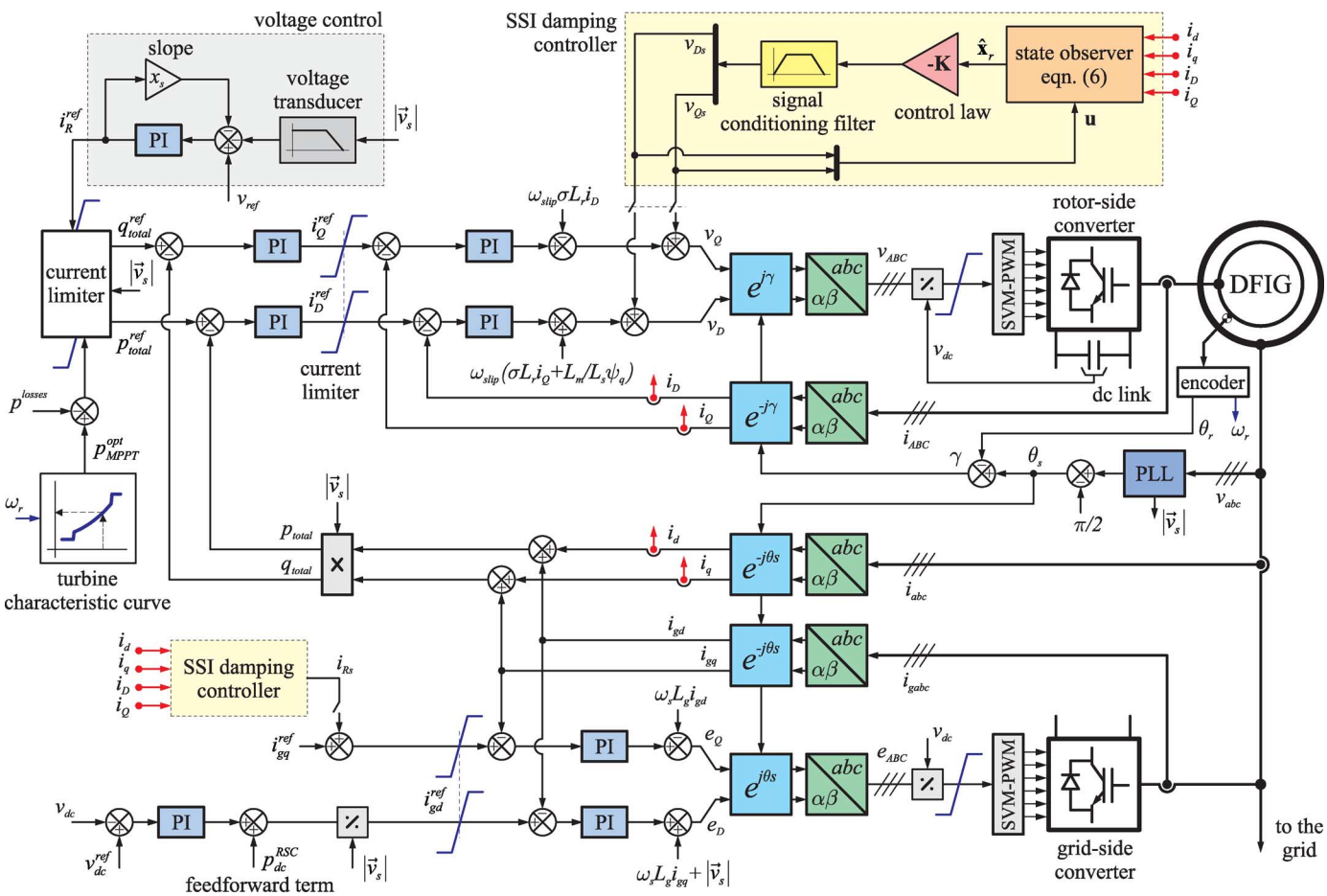

Fig. 3. DFIG vector control and place where the supplementary SSI damping control signals are added.

using the GSC active current loop. The control of the DFIG currents was achieved through the classical vector control based on PI structures in the d-q reference frame with feed-forward decoupling terms [39], [41], [42], whereas the synchronization was accomplished using the phase-locked loop presented in [43] and [44].

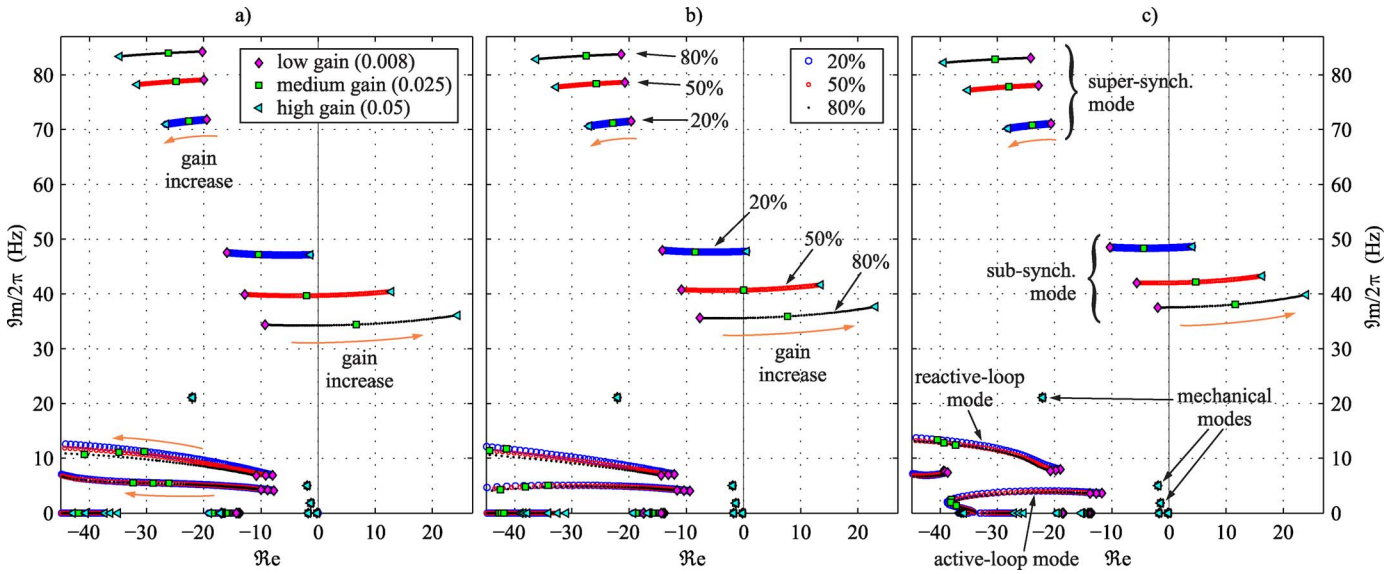

Fig. 4. Displacement of the eigenvalues when the gain of the rotor current control is varied, considering different cases of series compensation levels and wind speeds. a) High wind speed (maximum generated power). b) Medium wind speed. c) Low wind speed (minimum generated power).

IV. Description of the SSI Phenomenon

A. SSI Event in a DFIG Wind Farm and Case Study

In October 2009, in the southern ERCOT system (see left-side plot in Fig. 2), an SSI incident was reported when, following an N-1 contingency, a DFIG wind farm was radially connected to a series-compensated line. The 345-kV Ajo-Nelson Sharpe line was tripped after a single line-to-ground fault and, subsequently, the Zorillo wind farm became radially connected to the Rio Hondo series-compensated line. Immediately after the line outage, sub-synchronous growing currents and voltages were recorded, and in a short period of time, damages occurred in both series capacitor and wind turbine equipments [5].

To obtain a network configuration similar to the ERCOT system where this SSI event took place, the circuit breakers of the Ajo-Nelson Sharpe line were opened, due to a planned outage or a contingency, leaving the wind farm radially connected to the series-compensated line (see single-line diagram in Fig. 2). This case study is used to analyze the SSI phenomenon and assess the proposed controllers.

B. SSI Phenomenon in DFIG Wind Farms

Eigenvalues and modal analysis tools are used to analyze and understand the SSI phenomenon in DFIG wind farms connected to series-compensated lines. The presented results correspond to the case study in Fig. 2 with the Ajo-Nelson Sharpe line out of service, and without the SSI damping control (base scenario). The system eigenvalues are shown in Fig. 4(a), (b), and (c) for high, medium, and low wind speeds, respectively. These figures show the movement of the eigenvalues when the gain of the rotor current PI control, with the standard form $G_{PI}(s) = K(1 + 1/T_i s)$, is varied from a low to a high value [arrows in Fig. 4(a) mark the direction of the gain increase]. Each figure presents three series compensation levels, namely: 20% (large blue circle markers), 50% (red circle markers), and 80% (small black circle markers). Using the participation factors, we identify the eigenvalues associated with the super- and sub-synchronous modes, active and reactive power control loops, and mechanical modes of the wind turbine [to avoid label overlapping only indicated in Fig. 4(c)].

Studying the eigenvalue movement of Fig. 4, the following remarks can be made. First, the main instability problem is caused by the rotor current controller, which pushes the sub-synchronous mode to the right-side plane when its control gain is increased; this is a clear SSCI phenomenon. Second, when the wind speed is reduced or the series compensation level is increased, the sub-synchronous mode is destabilized, loosing its damping due to the IGE phenomenon. Third, the mechanical modes of the wind turbine are practically not affected by the different parameter variations; therefore, at least for this case study, TI and SSTI phenomena are not evidenced. To summarize, the SSCI is the main cause of sub-synchronous instability in DFIG wind farms connected to series-compensated lines. There is also an overlapped IGE phenomenon, which exacerbates the instability, but it does not seem to be the dominant effect [23].

Some authors propose to diminish the rotor current control gain to reduce the SSI effects; however, this can deteriorate the DFIG control bandwidth and make it more difficult to fulfill the fault-ride-through requirements of current grid codes [23]. In the rest of the article, we prefer to enhance the DFIG control with supplementary damping control signals to mitigate SSO without diminishing the rotor current control gain.

V. SSI Damping Control Design

The dynamics of the system and wind farm can be represented by a set of differential equations, $\dot{\mathbf{x}} = \mathbf{f}(\mathbf{x}, \mathbf{u})$ and $\mathbf{y} = \mathbf{h}(\mathbf{x}, \mathbf{u})$, where $\mathbf{x}$, $\mathbf{y}$, and $\mathbf{u}$ are the state, output, and input vectors of the system. The state vector consists of the dynamic variables of the electrical and mechanical states of the DFIG

wind turbine, vector control, converters, and equivalent electrical network. To avoid communication time-delays, we designed the SSI damping control by choosing the measurement output vector, $\mathbf{y} = [i_d \ i_q \ i_D \ i_Q]^T$, consisting of the local measurements of the d-q axis currents of the DFIG stator and rotor windings, which were already measured by the standard DFIG vector control.

In the analysis of the previous section, we observed that the rotor current control loop, which manages the rotor voltages, has a direct impact on the SSO damping. Therefore, these voltage control inputs are expected to have a high controllability of the sub-synchronous mode. The GSC reactive current can also be considered to damp SSO (as in a STATCOM approach). On the other hand, the GSC active current was discarded to damp SSO because this control loop is used to regulate the dc-link voltage. Consequently, we analyzed and compared two damping approaches with different control input vectors: one of them, $u_{gsc} = i_{Rs}$, was added to the reactive current reference of the GSC, and the other one, $\mathbf{u}_{rsc} = [v_{Ds} \ v_{Qs}]^T$, to the D-Q axis rotor voltages (see Fig. 3).

Model reduction is often applied to obtain a lower order model for the control design stage [45]. The following state-space representation of the reduced system model was obtained by using the balanced model truncation:

$$\dot{\mathbf{x}}_r = \mathbf{A}_r\mathbf{x}_r + \mathbf{B}_r\mathbf{u} \tag{4}$$

$$\mathbf{y} = \mathbf{C}_r\mathbf{x}_r \tag{5}$$

where the vector $\mathbf{x}_r \in \mathbb{R}^{n_r \times 1}$ represents the internal states of the reduced model, and n_r is the reduced model order. For details of the reduction methodology, see [46] and [47].

A MIMO state-space approach was chosen for the control design, so the control law was obtained by the state-feedback controller $\mathbf{u} = -\mathbf{K}\mathbf{x}_r$. The control gain $\mathbf{K} \in \mathbb{R}^{n_u \times n_r}$ was calculated based on an optimal quadratic technique (LQR) by minimizing the cost function $J = \int \left(\mathbf{y}^T\mathbf{Q}\mathbf{y} + \mathbf{u}^T\mathbf{R}\mathbf{u}\right) dt$[48]. This approach takes advantage of the multi-variable nature of the control system, and it is very simple to tune due to the physical interpretation of the design weighting matrices $\mathbf{Q}$ and $\mathbf{R}$, which were selected as a trade-off between the desired output deviations $(\mathbf{y})$ and the amount of control energy spent by the actuators $(\mathbf{u})$.

To implement the control law, the reduced states $\mathbf{x}_r$ are required, which do not have any physical meaning, and cannot be measured. To overcome this limitation, the internal states $\mathbf{x}_r$ were estimated from the measures $\mathbf{y}$ by means of a state observer (or software sensor) [48] as follows:

$$\dot{\hat{\mathbf{x}}}_r = \mathbf{A}_r\hat{\mathbf{x}}_r + \mathbf{B}_r\mathbf{u} + \mathbf{G}\left(\mathbf{y} - \mathbf{C}_r\hat{\mathbf{x}}_r\right) \tag{6}$$

where $\hat{\mathbf{x}}_r$ are the estimated states, and $\mathbf{G} \in \mathbb{R}^{n_r \times 4}$ is the observer gain matrix. By defining the estimation error $\mathbf{e} \triangleq \mathbf{x}_r - \hat{\mathbf{x}}_r$, the error dynamics can be written as $\dot{\mathbf{e}} = (\mathbf{A}_r - \mathbf{G}\mathbf{C}_r)\,\mathbf{e}$. Then, the matrix $\mathbf{G}$ can be designed using the Kalman filter approach, eigenvalue placement or optimal quadratic regulation; the latter was used in our design [48]. A signal-conditioning and filtering stage was included in the control output to allow damping signals to act only on the frequency range of interest.

In the case study, we considered the reduced model order $n_r = 11$, the weighting matrices $\mathbf{Q} = \left[\mathbf{I}^{2\times2}\, 0.1\mathbf{I}^{2\times2}\right]$, $\mathbf{R}_{rsc} = 65\mathbf{I}^{2\times2}$, and $R_{gsc} = 0.8$ for the control law, and $\mathbf{Q} = 20 \times 10^3\mathbf{I}^{n_r\times n_r}$ and $\mathbf{R} = \mathbf{I}^{4\times4}$ for the observer design. A block diagram showing the structure of the proposed SSI damping controller is presented at the top of Fig. 3.

VI. Performance Testing

Power system tests were performed using electromagnetic transient models from SimPowerSystems blockset of SIMULINK/MATLAB®. Nonlinear time-domain simulations included a wide range of dynamic phenomena, from the wind turbine mechanical system to power switching devices. On the other hand, in the modal analysis, we calculated the eigenvalues by writing the ordinary differential equations of each system component in the MATHEMATICA® software package, and the system eigenproperties were computed following the expressions given in [38].

A. Small-Signal Stability Analysis

Eigenvalue analysis was used to compare the performance and robustness of three cases: 1) classical vector control [called Base case, shown in Fig. 5(a)], 2) vector control plus the SSI damping controller acting on the GSC control [Control-A case, Fig. 5(b)], and 3) vector control plus the SSI damping controller on the RSC [Control-B case, Fig. 5(c)]. Although series capacitor compensations are usually fixed, the compensation level seen from the wind farm node can present some variations depending on whether certain parallel lines are connected or not. Fig. 5 shows the movement of the eigenvalues when the series compensation level is fully varied from 1% to 100%, considering four wind speed scenarios. A yellow star marker indicates the nominal 50% compensation level. An oscillating or unstable behavior is observed in the Base case with a 50% compensation level. In agreement with the previous analysis, in Fig. 5(a), a damping degradation of the sub-synchronous mode is also seen for lower wind speeds and higher compensation levels.

A good damping is obtained in the Control-A case around the nominal series compensation level, but it loses performance for high series compensation levels beyond the nominal point, where the controller was tuned [see Fig. 5(b)]. Finally, the Control-B case achieves a damping of the sub-synchronous mode higher than the Control-A case. A better robustness is also attained when the series compensation is moved far from the nominal point of 50% compensation [see Fig. 5(c)]. Therefore, from the small-signal stability point of view, the Control-B case presents a damping performance and robustness higher than the Control-A case.

B. Large-Signal Stability Analysis

The transient response of the system was evaluated by applying a 100-ms fault in the Ajo-Nelson Sharpe transmission line, followed by the line outage. We considered a 50% compensation level of the Rio Hondo-Lon Hill line, and a wind speed of 9.75 m/s. The under-study cases are shown in Fig. 6, namely: Base case (first column in Fig. 6), Control-A

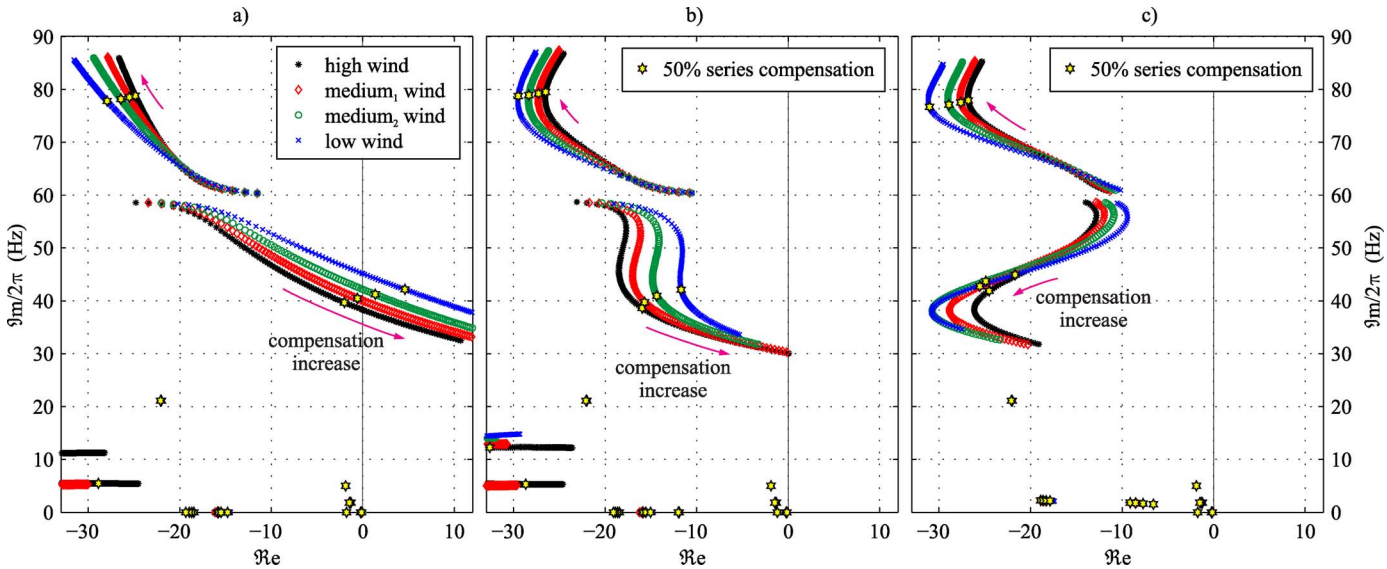

Fig. 5. Eigenvalues of the system when the series compensation level is varied from 1% to 100%, considering four wind speed scenarios. a) Base case. b) Control-A case. c) Control-B case.

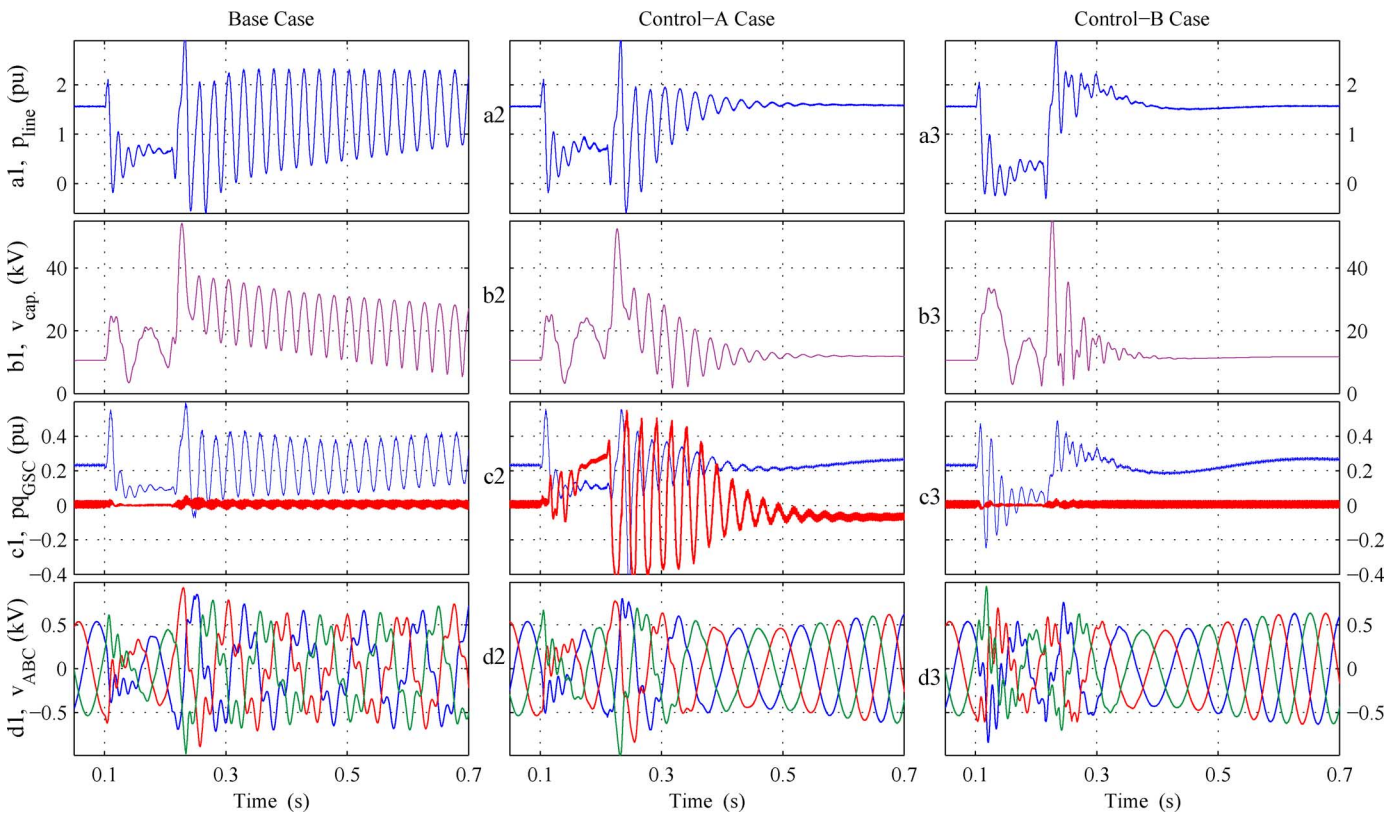

Fig. 6. Performance comparison of the Base, Control-A, and Control-B cases, considering a 50% compensation level and wind speed of 9.75 m/s. Plots (a1)-(a3): Line active power, (b1)-(b3): series capacitor voltage amplitude, (c1)-(c3): active (thin blue line) and reactive (thick red line) power injected by the GSC, (d1)-(d3): three-phase rotor voltages.

case (second column), and Control-B case (third column). In general, the Control-B case has a better damping performance than the Control-A case, but both controls can properly damp the SSO. The supplementary damping control action of the Control-A case causes significant reactive power excursion in the GSC [see Fig. 6(c2)], but the current is limited to the rated value. This excursion in the reactive power of the GSC is the control input or control action used by the SSI damping control to damp the SSO. This is a disadvantage of the Control-A case against the Control-B case, as the last one uses less control effort (*i.e.*, it slightly modifies the rotor voltage amplitude) [see Fig. 6(d3)] to accomplish the damping of the SSO. This is because the rotor voltage control input has a controllability index of the sub-synchronous mode higher than the reactive

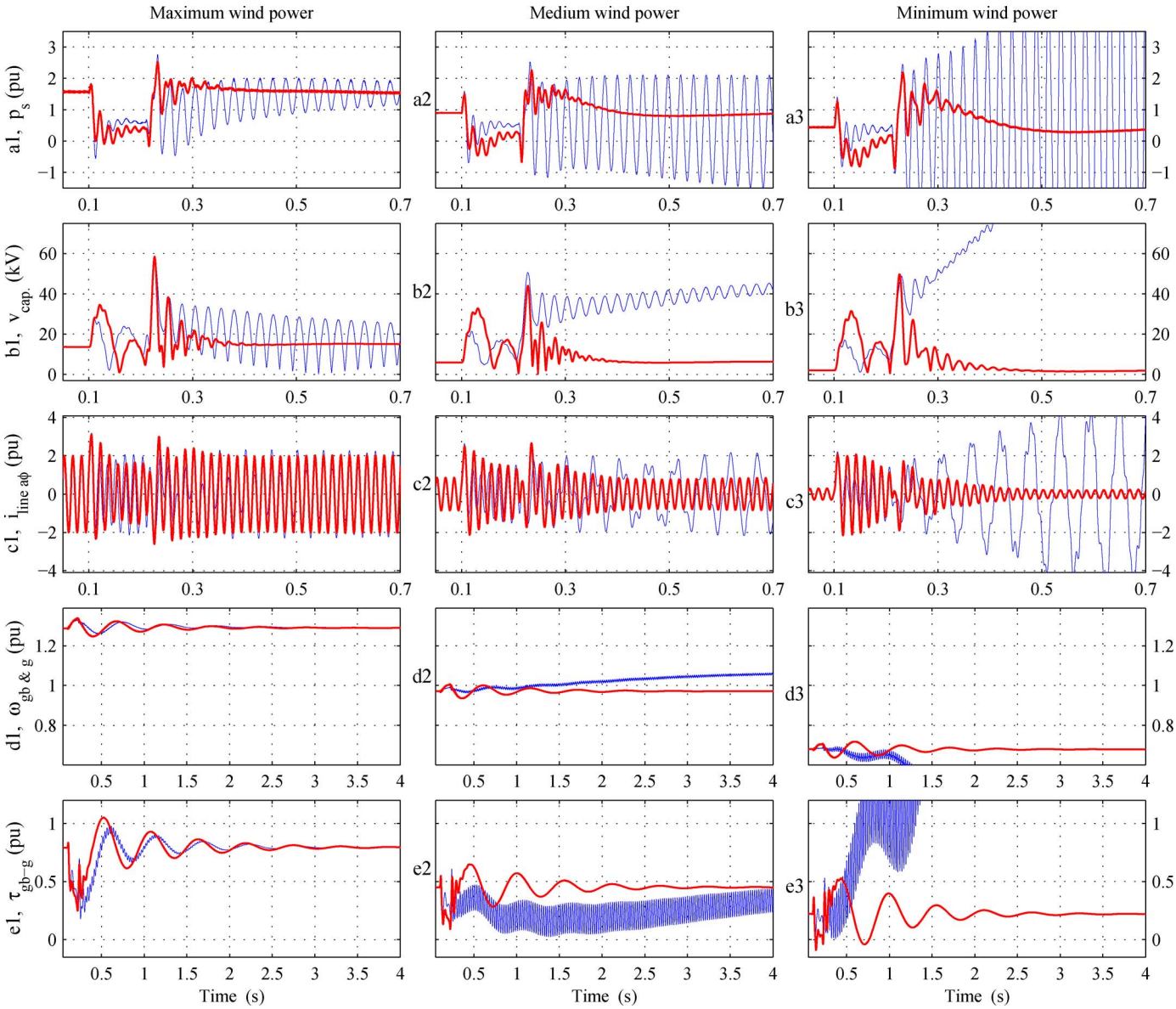

Fig. 7. Performance comparison of the Base case (thin blue line) against the Control-B case (thick red line) under different wind speed conditions. Plots (a1)-(a3): DFIG stator active power, (b1)-(b3): series capacitor voltage amplitude, (c1)-(c3): a-phase line current, (d1)-(d3): generator and gear-box speeds, (e1)-(e3): torque between the generator and gear-box stages.

current control input of the GSC. Therefore, the control action to damp the SSO required by the GSC damping control is larger than that for the RSC damping control. The higher effectiveness of the RSC control loop over the GSC control loop can be explained because it modifies the effective rotor resistance, which directly impacts on the SSO damping.

A test to assess the SSI damping control performance under different wind speed conditions is also presented. Nonlinear time-domain simulation results comparing several electrical and mechanical variables are shown in Fig. 7, where the same fault of the previous test was applied. In the Base case, the SSI phenomenon becomes more severe as the generated wind power lowers. However, in the Control-B case, we see a damped response for all wind speed conditions. Both electrical and mechanical variables increase their damping, which improves the delivered power quality and system stability margin, and reduces the drive-train mechanical stress as well.

Finally, a test using a 75% compensation level was accomplished to evaluate the control performance under a higher series compensation level (see Fig. 8). The results show that high damping and good robustness are achieved by the proposed strategy for different power system operating conditions.

VII. Conclusions

Recent events showed that SSI are a potential threat for DFIG wind farms particularly if, due to contingencies or planned outages, these wind farms operate radially in a series-compensated transmission system. To reduce the risk of SSI and enhance the power system operation, we proposed a control strategy which modifies the existing DFIG control systems by adding supplementary damping control signals. In this way, the installation of additional damping devices, such as FACTS or bypass filters, are avoided, and a cheaper and quicker solution

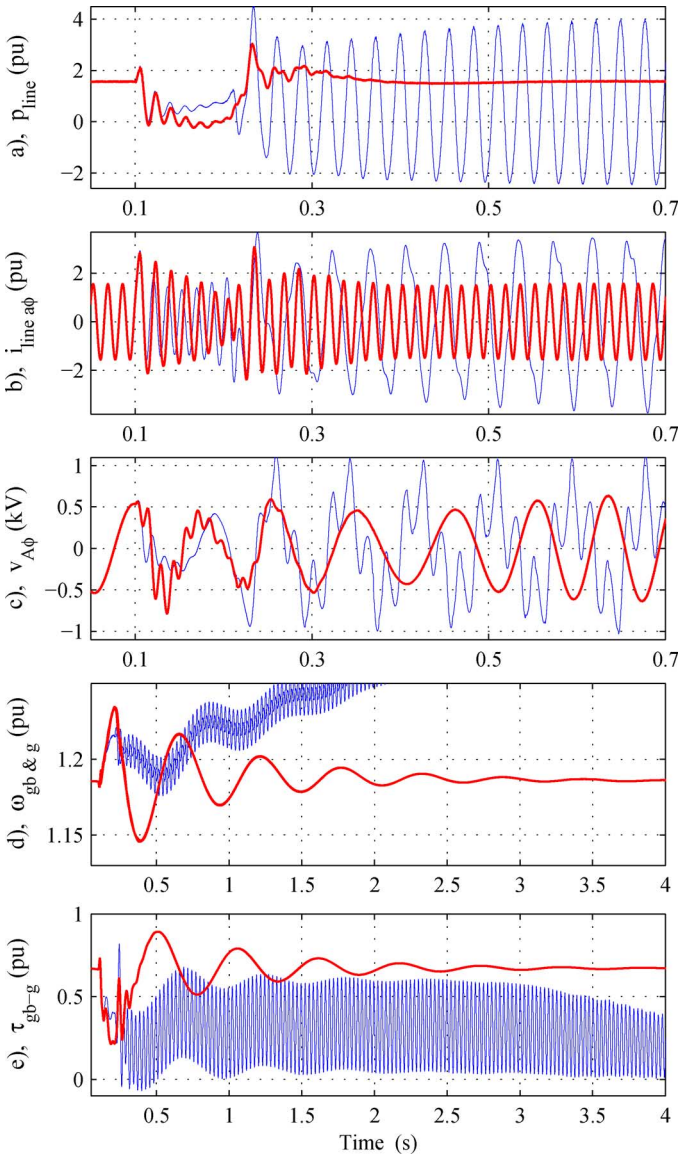

Fig. 8. Test using a 75% compensation level and wind speed of 9.75 m/s. Base case (thin blue line) and Control-B case (thick red line). Plots (a): Line active power, (b): a-phase line current, (c): a-phase rotor voltage, (d): generator and gear-box speeds, (e): torque between the generator and gear-box stages.

is achieved. Besides, the auxiliary damping control was integrated to DFIG vector control maintaining the well-known PI control structures, becoming more acceptable for system operators. Two SSI damping control approaches were analyzed and compared; the first one acts on the GSC control loop, and the second one uses the RSC control loop. Both controllers were designed using a state-space methodology able to manage several measurements and control inputs. The RSC damping control presented a higher damping performance, lower actuator control effort, and better robustness against changes in the operating conditions compared with the GSC damping control. Due to space limitations, we could not include further tests and data, but the obtained results showed that encouraging SSO damping improvements over a wide range of operating conditions can be obtained when supplementary controls are integrated to the classical DFIG vector controls.

REFERENCES

[1] E. Larsen, "Wind generators and series-compensated AC transmission lines," in *Proc. IEEE PES Transm. Distrib. Conf. Expo.*, 2012, pp. 1–4.

[2] D. Suriyaarachchi, U. Annakkage, C. Karawita, and D. Jacobson, "A procedure to study sub-synchronous interactions in wind integrated power systems," *IEEE Trans. Power Syst.*, vol. 28, no. 1, pp. 377–384, Feb. 2013.

[3] R. Varma, S. Auddy, and Y. Semsedini, "Mitigation of subsynchronous resonance in a series-compensated wind farm using FACTS controllers," *IEEE Trans. Power Del.*, vol. 23, no. 3, pp. 1645–1654, Jul. 2008.

[4] A. Moharana and R. Varma, "Subsynchronous resonance in single-cage self-excited-induction-generator-based wind farm connected to series-compensated lines," *IET Gener., Transm., Distrib.*, vol. 5, pp. 1221–1232, Dec. 2011.

[5] J. Daniel *et al.*, ERCOT CREZ Reactive Power Compensation Study, ABB Inc., Power Systems Division, Grid Systems Consulting, 2010, E3800-PR-00.

[6] L. C. Gross, "Sub-synchronous grid conditions: New event, new problem, and new solutions," in *Proc. Western Protective Relay Conf.*, 2010, pp. 1–5.

[7] J. Adams, C. Carter, and S.-H. Huang, "ERCOT experience with sub-synchronous control interaction and proposed remediation," in *Proc. IEEE PES Transm. Distrib. Conf. Expo.*, 2012, pp. 1–5.

[8] D. Kidd and P. Hassink, "Transmission operator perspective of sub-synchronous interaction," in *Proc. IEEE PES Transm. Distrib. Conf. Expo.*, 2012, pp. 1–3.

[9] M. Bongiorno, A. Petersson, and E. Agneholm, "The impact of wind farms on subsynchronous resonance in power systems," *Elforsk rapport 11:29*, 2011.

[10] K. Narendra, D. Fedirchuk, R. Midence, N. Zhang, A. Mulawarman, P. Mysore, and V. Sood, "New microprocessor based relay to monitor and protect power systems against sub-harmonics," in *Proc. IEEE Elect. Power and Energy Conf. (EPEC'11)*, 2011, pp. 438–443.

[11] R. Varma and A. Moharana, "SSR in double-cage induction generator-based wind farm connected to series-compensated transmission line," *IEEE Trans. Power Syst.*, vol. 28, no. 3, pp. 2573–2583, Aug. 2013.

[12] A. Ostadi, A. Yazdani, and R. Varma, "Modeling and stability analysis of a DFIG-based wind-power generator interfaced with a series-compensated line," *IEEE Trans. Power Del.*, vol. 24, no. 3, pp. 1504–1514, Jul. 2009.

[13] L. Fan, R. Kavasseri, Z. L. Miao, and C. Zhu, "Modeling of DFIG-based wind farms for SSR analysis," *IEEE Trans. Power Del.*, vol. 25, no. 4, pp. 2073–2082, Oct. 2010.

[14] S. Atayde and A. Chandra, "Multiple machine representation of DFIG based grid-connected wind farms for SSR studies," in *Proc. Annu. Conf. IEEE Ind. Electron. Soc., IECON*, 2011, pp. 1468–1473.

[15] Z. Miao, "Impedance-model-based SSR analysis for type 3 wind generator and series-compensated network," *IEEE Trans. Energy Convers.*, vol. 27, no. 4, pp. 984–991, Dec. 2012.

[16] Y. Cheng, M. Sahni, D. Muthumuni, and B. Badrzadeh, "Reactance scan crossover-based approach for investigating SSCI concerns for DFIG-based wind turbines," *IEEE Trans. Power Del.*, vol. 28, no. 2, pp. 742–751, Apr. 2013.

[17] Z. Miao, "Impact of unbalance on electrical and torsional resonances in power electronic interfaced wind energy systems," *IEEE Trans. Power Syst.*, vol. 28, no. 3, pp. 3105–3113, Aug. 2013.

[18] M. El-Moursi, B. Bak-Jensen, and M. Abdel-Rahman, "Novel STATCOM controller for mitigating SSR and damping power system oscillations in a series compensated wind park," *IEEE Trans. Power Electron.*, vol. 25, no. 2, pp. 429–441, 2010.

[19] S. Golshannavaz, M. Mokhtari, and D. Nazarpour, "SSR suppression via STATCOM in series compensated wind farm integrations," in *Proc. Iranian Conf. Elect. Eng. (ICEE'11)*, 2011, pp. 1–6.

[20] L. Fan, C. Zhu, Z. Miao, and M. Hu, "Modal analysis of a DFIG-based wind farm interfaced with a series compensated network," *IEEE Trans. Energy Convers.*, vol. 26, no. 4, pp. 1010–1020, Dec. 2011.

[21] L. Fan and Z. Miao, "Mitigating SSR using DFIG-based wind generation," *IEEE Trans. Sustain. Energy*, vol. 3, pp. 349–358, Jul. 2012.

[22] C. Zhu, L. Fan, and M. Hu, "Control and analysis of DFIG-based wind turbines in a series compensated network for SSR damping," in *Proc. IEEE Power and Energy Soc. General Meeting*, 2010, pp. 1–6.

[23] G. Irwin, A. Jindal, and A. Isaacs, "Sub-synchronous control interactions between type 3 wind turbines and series compensated AC transmission systems," in *Proc. IEEE Power Energy Soc. General Meeting*, Jul. 2011, pp. 1–6.

[24] B. Badrzadeh, M. Sahni, Y. Zhou, D. Muthumuni, and A. Gole, "General methodology for analysis of sub-synchronous interaction in wind power plants," *IEEE Trans. Power Syst.*, vol. 28, no. 2, pp. 1858–1869, May 2013.
[25] T. Ackermann and R. Kuwahata, "Lessons learned from international wind integration studies," *AEMO Wind Integration WP4(A). Commissioned by Australian Energy Market Operator*, 2011.
[26] IEEE Committee Report, "Reader's guide to subsynchronous resonance"," *IEEE Trans. Power Syst.*, vol. 7, no. 1, pp. 150–157, Feb. 1992.
[27] P. Pourbeik, R. Koessler, D. Dickmander, and W. Wong, "Integration of large wind farms into utility grids (Part 2 – Performance issues)," in *Proc. IEEE Power Eng. Soc. General Meeting*, 2003, vol. 3, pp. 1520–1525.
[28] K. R. Padiyar, *Power System Dynamics: Stability and Control*, 2nd ed. Hyderabad, India: BS Publications, 2008.
[29] C. Zhu, M. Hu, and Z. Wu, "Parameters impact on the performance of a double-fed induction generator-based wind turbine for subsynchronous resonance control," *IET Renew. Power Gener.*, vol. 6, no. 2, pp. 92–98, 2012.
[30] G. Irwin, A. Isaacs, and D. Woodford, "Simulation requirements for analysis and mitigation of SSCI phenomena in wind farms," in *Proc. IEEE PES Transm. Distrib. Conf. Expo.*, 2012, pp. 1–4.
[31] A. E. Leon and J. A. Solsona, "Performance improvement of full-converter wind turbines under distorted conditions," *IEEE Trans. Sustain. Energy*, vol. 4, pp. 652–660, Jul. 2013.
[32] A. E. Leon, M. F. Farias, P. E. Battaiotto, J. A. Solsona, and M. I. Valla, "Control strategy of a DVR to improve stability in wind farms using squirrel-cage induction generators," *IEEE Trans. Power Syst.*, vol. 26, no. 3, pp. 1609–1617, Aug. 2011.
[33] P. C. Krause, *Analysis of Electric Machinery*. New York, NY, USA : McGraw-Hill, 1995.
[34] V. Blasco and V. Kaura, "A new mathematical model and control of a three-phase AC-DC voltage source converter," *IEEE Trans. Power Electron.*, vol. 12, no. 1, pp. 116–123, Jan. 1997.
[35] J. Slootweg, S. de Haan, H. Polinder, and W. Kling, "General model for representing variable speed wind turbines in power system dynamics simulations," *IEEE Trans. Power Syst.*, vol. 18, no. 1, pp. 144–151, Feb. 2003.
[36] S. Muyeen, M. Ali, R. Takahashi, T. Murata, J. Tamura, Y. Tomaki, A. Sakahara, and E. Sasano, "Comparative study on transient stability analysis of wind turbine generator system using different drive train models," *IET Renew. Power Gener.*, vol. 1, pp. 131–141, Jun. 2007.
[37] S. Papathanassiou and M. Papadopoulos, "Mechanical stresses in fixed-speed wind turbines due to network disturbances," *IEEE Trans. Energy Convers.*, vol. 16, no. 4, pp. 361–367, Dec. 2001.
[38] P. Kundur, *Power System Stability and Control*. New York, NY, USA: McGraw-Hill, 1994.
[39] R. Pena, J. Clare, and G. Asher, "Doubly fed induction generator using back-to-back PWM converters and its application to variable-speed wind-energy generation," *IEE Proc. Elect. Power Appl.*, vol. 143, pp. 231–241, May 1996.
[40] J. Martinez, P. Kjar, P. Rodriguez, and R. Teodorescu, "Comparison of two voltage control strategies for a wind power plant," in *Proc. IEEE/PES Power Systems Conf. Expo.*, Mar. 2011, pp. 1–9.
[41] B. Hopfensperger, D. Atkinson, and R. Lakin, "Stator-flux-oriented control of a doubly-fed induction machine with and without position encoder," *IEE Proc. Elect. Power Appl.*, vol. 147, pp. 241–250, Jul. 2000.
[42] A. Tapia, G. Tapia, J. X. Ostolaza, and J. R. Sáenz, "Modeling and control of a wind turbine driven doubly fed induction generator," *IEEE Trans. Energy Convers.*, vol. 18, no. 2, pp. 194–204, Jun. 2003.
[43] V. Kaura and V. Blasko, "Operation of a phase locked loop system under distorted utility conditions," *IEEE Trans. Ind. Appl.*, vol. 33, no. 1, pp. 58–63, Jan.–Feb. 1997.
[44] S.-K. Chung, "A phase tracking system for three phase utility interface inverters," *IEEE Trans. Power Electron.*, vol. 15, pp. 431–438, May 2000.
[45] A. E. Leon and J. A. Solsona, "Power oscillation damping improvement by adding multiple wind farms to wide-area coordinating controls," *IEEE Trans. Power Syst.*, vol. 29, no. 3, pp. 1356–1364, May 2014.
[46] M. Safonov and R. Chiang, "A Schur method for balanced-truncation model reduction," *IEEE Trans. Autom. Control*, vol. 34, pp. 729–733, Jul. 1989.
[47] A. E. Leon, J. M. Mauricio, and J. A. Solsona, "Subsynchronous resonance mitigation using variable-speed wind energy conversion systems," *IET Gener., Transm., Distrib.*, vol. 7, pp. 511–525, May 2013.
[48] K. Ogata, *Modern Control Engineering*. Englewood Cliffs, NJ, USA: Prentice Hall, 1997.

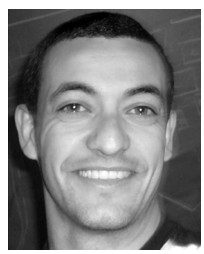

Andres E. Leon (S'05–M'13) received the B.S. degree in electrical engineering from the Universidad Nacional del Comahue, Neuquén, Argentina, in 2005, and the Ph.D. degree in control systems from the Universidad Nacional del Sur, Bahía Blanca, Argentina, in 2011.

Since 2012, he has been with the National Scientific and Technical Research Council (CONICET) as a Researcher. He is currently working at the Research Institute of Electrical Engineering "Alfredo Desages" (IIIE), Argentina. His primary areas of interest are power system control and wind energy conversion systems.

Jorge A. Solsona (SM'04) received the electronics engineer and Dr. degrees from the Universidad Nacional de La Plata, La Plata, Argentina, in 1986 and 1995, respectively.

Currently, he is with the Instituto de Investigaciones en Ingeniería Eléctrica Alfredo Desages (IIIE), Departamento de Ingeniería Eléctrica y de Computadoras, Universidad Nacional del Sur, Bahía Blanca, Argentina, and CONICET, where he is involved in teaching and research on control theory and its applications to electromechanical systems.